Biophysics Reviews REVIEW pubs.aip.org/aip/bpr

On the reversibility of amyloid fibril formation

Cite as: Biophysics Rev. **6**, 011303 (2025); doi: 10.1063/5.0236947
Submitted: 2 September 2024 · Accepted: 31 December 2024 ·
Published Online: 29 January 2025

Tinna Pálmadóttir,[1] Josef Getachew,[1] Lei Ortigosa-Pascual,[1] Emil Axell,[1] Jiapeng Wei,[2] Ulf Olsson,[3] Tuomas P. J. Knowles,[2,a)] and Sara Linse[1,a)]

AFFILIATIONS

[1]Biochemistry and Structural Biology, Lund University, Lund, Sweden
[2]Yusuf Hamied Chemistry Department, University of Cambridge, Cambridge, United Kingdom
[3]Physical Chemistry, Lund University, Lund, Sweden

Note: This paper is part of the BPR Special Topic on Biomolecular Phase Transitions and the Mechanochemical Control of Cells in Health & Disease.
[a)]**Authors to whom correspondence should be addressed:** tpjk2@cam.ac.uk and sara.linse@biochemistry.lu.se

ABSTRACT

Amyloids are elongated supramolecular protein self-assemblies. Their formation is a non-covalent assembly process and as such is fully reversible. Amyloid formation is associated with several neurodegenerative diseases, and the reversibility is key to maintaining the healthy state. Reversibility is also key to the performance of fibril-based biomaterials and functional amyloids. The reversibility can be observed by a range of spectroscopic, calorimetric, or surface-based techniques using as a starting state either a supersaturated monomer solution or diluted fibrils. Amyloid formation has the characteristics of a phase transition, and we provide some basic formalism for the reversibility and the derivation of the solubility/critical concentration. We also discuss conditions under which the dissociation of amyloids may be so slow that the process can be viewed as practically irreversible, for example, because it is slow relative to the experimental time frame or because the system at hand contains a source for constant monomer addition.

TABLE OF CONTENTS

Significance statement: Reversibility of amyloid formation is an often ignored but fundamental physicochemical property, like in all non-covalent assembly processes. Reversibility is key to maintaining the healthy state in body fluids and cells with a plethora of aggregation-prone peptides and proteins. Reversibility is also key to the performance of fibril-based biomaterials and functional amyloids.

I. INTRODUCTION

Amyloid fibrils are highly stable supramolecular protein self-assemblies, which can be formed from many different types of peptide and proteins and which are involved in both biological function and malfunction. One of the main structural characteristics of amyloids are their ordered fibril core, consisting of β-strands arranged perpendicular to the fibril axis (Eanes and Glenner, 1968; Jahn *et al.*, 2010; Colvin *et al.*, 2016; Iadanza *et al.*, 2018; and Ke *et al.*, 2020). The misfolding and self-assembly of proteins into amyloid fibrils is linked to many pathological conditions, such as Alzheimer, Parkinson, Hungtingon's, Prion diseases, and type II diabetes (Jarrett *et al.*, 1993; Selkoe, 2004; Chiti and Dobson, 2006; Lansbury and Lashuel, 2006; Sipe *et al.*, 2012; Chiti and Dobson, 2017; and Ke *et al.*, 2020). We expect amyloids to follow the same physicochemical principles as for self-assembly in general, including all peptide and protein fibrils assembled as extended β-sheets, and the principles discussed in this work refer to all such assemblies. Like other non-covalent self-assembly processes, protein amyloid formation is reversible. Reversibility in self-assembly is well established through equilibrium phase diagrams in a range of systems, including surfactant and lipid self-assembly (Laughlin, 1994; Evans and Wennerström, 1999). It is also fundamentally linked to thermodynamic equilibrium (Tolman, 1925). Examples from reversible protein and peptide self-assembly include the formation of virus capsid shells (Comas-Garcia *et al.*, 2014) and peptide nanotubes (Narayanan *et al.*, 2021). More generally, from a statistical mechanics point of view, for any forward process, there has to exist, in principle, also a reverse process. At equilibrium, the rates of both the forward and reverse transformation are equal; out of equilibrium, however, their rates can be dramatically different. The question of reversibility, therefore, at a fundamental level, relates to the question of whether, in a given transformation, the reverse rate is relevant and observable. However, due to the common description of the amyloid formation process as irreversible, we discuss here under what conditions the reverse process, amyloid disassembly is relevant. Specifically, we ask under what circumstances the reversibility of amyloid formation is readily observable and under what conditions the situation can be viewed as practically irreversible, although the underlying amyloid-formation process is of course still reversible.

A distinction, which can be helpful in practice, is to consider whether the amyloid formation process is thermodynamically or kinetically controlled. Under thermodynamic control, the system reaches the same end point, the (local) thermodynamic equilibrium regardless of its starting state (Fig. 1). By contrast, under kinetic control, the final equilibrium state is not reached on the timescale of the experiment, and thus, the long-time state can vary depending on preparation route, over some defined time-frame.

A. Amyloid formation as a phase separation process

Molecular self-assembly transforms elementary building blocks into organized structures and exhibits features of true phase transitions as structure size increases ($N \to \infty$). This behavior, seen in systems like self-assembling amphiphiles, leads to abrupt changes in solution properties at critical concentrations. Linear self-assembling systems, including amyloid, show similar behavior under conditions favoring large aggregates; amyloid fibrils may contain thousands of monomers. Such assembly processes are typically characterized by a critical aggregation concentration (c_c) equal to the solubility (S). Even at finite aggregate sizes, these transformations have many features in common

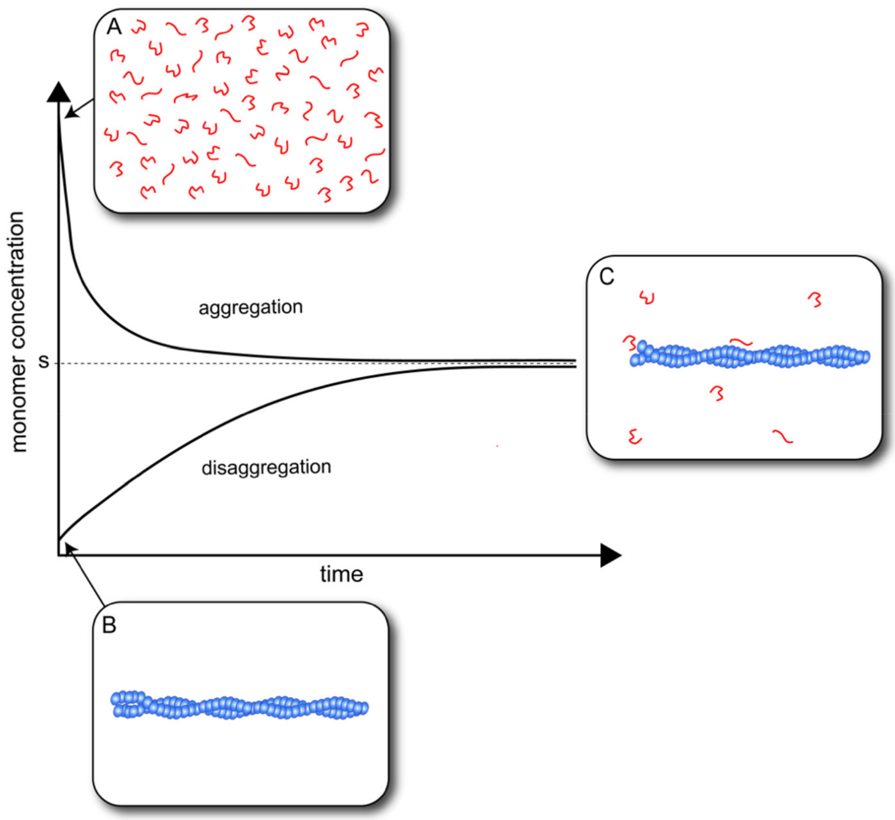

FIG. 1. Reversible amyloid formation under thermodynamic control. Irrespective of the starting state having a surplus of monomers (above the solubility limit) (a) or fibrils (below the solubility limit) (b), the same end state is reached over time, where the monomer concentration equals the solubility (S) (the critical concentration) of the protein (c), although it may take more time to reach state (c) from (b) than from (a). In all panels, free monomers are drawn as curved red lines and monomers in fibrils as blue ellipsoids.

with true thermodynamic phase transitions and become physical phase transitions for infinitely large aggregates. (Hellstrand *et al.*, 2010; Michaels *et al.*, 2023; and Goto *et al.*, 2024). Under such conditions, the critical concentration, c_c, is the ratio of the rate constant of monomer addition to the aggregates, k_+ and the rate constant of the inverse process of monomer detachment from aggregates k_{off},

$$c_c = \frac{k_{off}}{k_+}. \tag{1}$$

Interestingly, Eq. (1) has a simple interpretation in terms of mass balance for the equilibrium $\mathrm{F} \rightleftharpoons \mathrm{F} + \mathrm{m}$, where m is a free monomer and F is a fibril end when assuming that the chemical potential of the monomers in fibrils is concentration independent, as would be expected for a molecule in a pure solid phase (Fig. 2). This observation further highlights the analogies between amyloid formation and conventional phase transitions. The equilibrium parameter of interest is the solubility S, i.e., the monomer concentration that coexists with aggregates at equilibrium (Evans and Wennerström, 1999).

$$S = \exp\left\{\frac{\mu_a^o - \mu_m^o}{RT}\right\}. \tag{2}$$

Here, μ_a^o is the protein standard chemical potential in aggregates and μ_m^o is its standard chemical potential as free monomers in solution. The solubility S is equal to the critical concentration c_c.

Equation (2) is obtained by considering that a dilute monomer solution of concentration $[m]$, has a chemical potential $\mu_m = \mu_m^0 + RT\ln[m]$, while in the aggregated "solid" the corresponding chemical potential is constant, $\mu_a = \mu_a^0$, because there is no entropy of mixing. In an equilibrium with the coexistence of monomer and aggregates, $\mu_a = \mu_m$, leading to Eq. (2) where $[m] = S$.

It is important to note that the chemical potential in the monomeric state depends on the concentration $[m]$, with thermodynamic coexistence between monomers and fibrils being characterized by $[m] = S$. Amyloid formation displays an abrupt shift where most molecules end up in aggregates once the critical concentration (solubility) is surpassed. In a supersaturated solution $[m] > S$, and fibrils may form and grow. In undersaturated solutions, on the other hand, where $[m] < S$, existing fibrils are expected to dissolve (see Fig. 1). It is, therefore, important to specify also the total protein concentration when comparing monomer and aggregate chemical potentials or free energy states in a free energy landscape (Balchin *et al.*, 2016; Adamcik and Mezzenga, 2018; Ke *et al.*, 2020; and Frey *et al.*, 2024). In Fig. 2, we illustrate the simplest example of a chemical potential diagram, where we compare free monomers and monomers in aggregates for an amyloid protein that is unfolded in its free state. As can be seen, the fibrils have a concentration-independent chemical potential, while the free monomer chemical potential increases with concentration, and the two curves cross at the solubility.

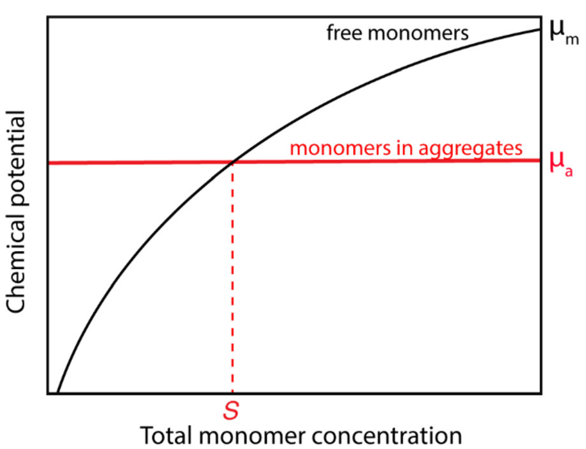

FIG. 2. Chemical potential. The concentration-dependent chemical potential of free monomers (black) is equal to the concentration-invariant chemical potential of monomers in aggregates (red) at the solubility (S), sometimes also referred to as the critical concentration (c_c).

B. Assembly pathway

If we consider the assembly pathway, the simultaneous condensation of very many monomers is highly unlikely, and instead, the process may occur by monomer addition to existing aggregates of various sizes. In addition to the aggregation number, the aggregates have internal degrees of freedom associated with the structure. Indeed, high molecular weight amyloid aggregates are highly ordered and β-sheet rich, while the smaller aggregates, often referred to as oligomers, are structurally distinct from the amyloid fibril structure, relatively less structured, less β-sheet rich, less stable, and often with more hydrophobic surfaces (Lendel *et al.*, 2014; Kjaergaard *et al.*, 2018; Lee *et al.*, 2018; and Dear *et al.*, 2020). It is typically only the highly ordered β-sheet rich aggregates that are able to grow through monomer elongation to very large sizes. Aggregates that have not undergone this structural conversion to the amyloid form remain in the solution phase (Frackowiak *et al.*, 1994). Oligomers have lower growth rate compared to aggregates after nucleation (Dear *et al.*, 2020) but may undergo this structural conversion step at which the aggregate structure abruptly changes into a structure that can be called a critical nucleus (the smallest subunit of the aggregated phase) (Michaels *et al.*, 2020) (Fig. 3). Critical nuclei can further grow into large amyloid fibril structures, forming a separate discontinuous phase that may precipitate or remain in colloidal suspension for at least some time.

Investigations of the amyloid formation processes have revealed in many cases a double nucleation mechanism, i.e., with primary nucleation from monomers only as well as secondary nucleation in the presence of aggregates (Fig. 3). Examples include the peptides and proteins IAPP, Aβ42, Aβ40, α-synuclein, and tau (Padrick and Miranker, 2002; Rodriguez Camargo *et al.*, 2021a; Cohen *et al.*, 2013; Meisl *et al.*, 2014; Buell *et al.*, 2014; Rodriguez Camargo *et al.*, 2021b; Ruschak and Miranker, 2007; Foderà *et al.*, 2008, and Gaspar *et al.*, 2017). As for any nucleated process, the free energy barrier for elongation (growth) is lower than the free energy barrier for nucleation (Zimm and Bragg, 1959; Lifson and Roig, 1961). Temperature-dependent studies have been performed to quantify this difference as well as the difference between the barriers for primary and secondary nucleation in the case of Aβ42 (Cohen *et al.*, 2018) and IAPP (Ruschak and Miranker, 2007).

Aggregation curves typically display a lag phase, a steep transition, and a final plateau (Jarrett and Lansbury, 1993; Arosio *et al.*, 2015). During the lag phase, the concentration of fibrils, $[m_f]$, grows almost exponentially, according to (Arosio *et al.*, 2014)

$$[m_f] = A\{\cosh(\kappa t) - 1\}. \tag{3}$$

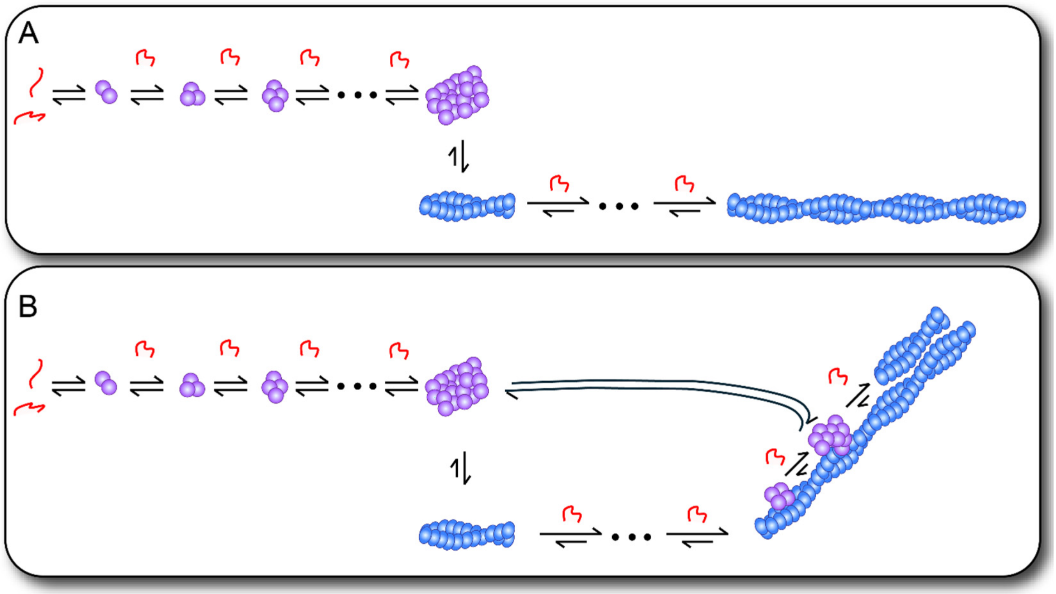

FIG. 3. Schematic description of reversible amyloid formation. (a) An amyloid formation process with primary nucleation and elongation steps. (b) An amyloid formation process with primary nucleation, secondary nucleation, and elongation steps. In both panels, free monomers are drawn as curved red lines, monomers in non-nucleated aggregates as purple spheres, and monomers in nucleated fibrils as blue ellipsoids. In the second case, it is not resolved whether conversion from non-nucleated to nucleated aggregates happens on the fibril surface or in solution, or both, and we, therefore, depict both options in this cartoon.

For a typical 100 μl sample of low μM concentration of Aβ42, the first fibrils form within a few ms (Arosio *et al.*, 2015) and can be detected after a few minutes, using cryo-TEM and filter trap methods (Arosio *et al.*, 2014). The length of the lag phase may be defined in several ways, but a practical approach is to define the end of the lag phase as the point in time at which the fibril concentration has reached a high enough value to be detected by bulk methods, which is typically around 1% of the final fibril concentration (Cohen *et al.*, 2013). Importantly, all microscopic processes, i.e., all nucleation and growth processes, occur during all stages of the process and with full reversibility, albeit with different net rates during different stages of the process, with nucleation rate approaching zero at long times (Arosio *et al.*, 2015).

Although the detailed aggregation process occurs through multiple steps (Fig. 3), all steps proceed at balanced rates at equilibrium such that the net flux is zero. In other words, the reaction is fully reversible and if an equilibrium is reached, there is no longer a net consumption of monomers. At equilibrium, the rate of monomers going from solution to aggregates is the same as the rate of monomers going from aggregates back into solution, and the process is ongoing all the time with full reversibility. To measure the forward or backward rate, the system needs, however, to be taken out of equilibrium. This can be achieved through dilution of fibrils or through the creation of a supersaturated monomer solution (Fig. 1). The approach to equilibrium can then be followed by methods that measure the monomer or fibril concentration, or both, e.g., by optical or NMR spectroscopy, quartz crystal microbalance or surface plasmon resonance techniques, scattering or filter-trap methods (Wetzel, 2006; White *et al.*, 2009; Buell *et al.*, 2012; Buell, 2019; Buell, 2022; Arosio *et al.*, 2014; Gaspar *et al.*, 2017; Brännström *et al.*, 2018; and Eves *et al.*, 2021), or methods monitoring the process of formation or dissociation, e.g., isothermal titration calorimetry (Kardos *et al.*, 2004; Koder Hamid *et al.*, 2020) and differential scanning calorimetry (Morel *et al.*, 2010). While the forward rates of monomer consumption and fibril formation are relatively easy to quantify, measurements of the backward rates may face a formidable experimental challenge under conditions of slow dissociation.

C. Modeling reversible self-assembly

Although there are most often more than one monomer per plane in a fibril, the elongation and shrinkage of fibrillar aggregates are well-described by monomer addition and monomer dissociation, respectively. The same can be assumed for oligomeric aggregates and a model can be built as an infinite number of equilibria as follows:

$$f(j) + m \overset{K_o}{\rightleftharpoons} f(j+1), \tag{4}$$

where $f(j)$ is the number concentration of j-mers. The equilibrium constant,

$$K_o = [f(j+1)]/[f(j)][m] = k_{+,o}/k_{off,o} = e^{-\Delta G^o/k_B T}, \tag{5}$$

where $k_{+,o}$ is the association rate constant and $k_{off,o}$ is the dissociation rate constant of monomers to and from the oligomer $[m]$ is the free monomer concentration, ΔG^o is the standard free energy difference between free monomer and monomer in an oligomer, k_B is the Boltzmann constant, and T is temperature. The oligomer mass concentration $[m_o]$ summed over all oligomer sizes, j, starting from $j=2$ equals

$$[m_o] = \sum_{j=2} j[f(j)] = \frac{[m]}{(1-K_o[m])^2} - [m]. \tag{6}$$

In the isodesmic model, all K_o values are identical. However, for amyloid proteins, at least two classes of aggregates are formed. In addition to the small aggregates, oligomers, with a lower stability, there are larger ones, fibrils, with a higher stability. We can, thus, assume a higher value of the equilibrium constant for the large compared to small aggregates, i.e., the system displays positive cooperativity as the aggregate grows. This behavior can, in the simplest case, be described using two equilibrium constants, K_f and K_o, where $K_f = e^{-\Delta G_f^o/K_B T}$ is the monomer binding constant for the fibril ends, and K_o is the monomer binding constant for the oligomers, with $K_f > K_o$. For the nucleus size n_c, the fibril mass concentration summed over all fibril sizes, $j \geq n_c$, equals

$$[m_f] = \sum\nolimits_{j \geq n_c} j[f(j)]. \tag{7}$$

The total monomer concentration takes the following form:

$$\begin{aligned} [m]_{tot} &= [m] + [m_o] + [m_f] \\ &= [m]/(1 - K_o[m])^2 + \sigma \frac{(K_f[m])^{n_c}}{(1 - K_f[m])^2} \\ &\quad \times \left[n_c K_f^{-1} + (1 - n_c)[m]\right], \end{aligned} \tag{8}$$

where $\sigma = \gamma (K_o/K_f)^2 \ll 1$ and γ is related to the structure of polymer. A value of $\gamma = 0.01$ represent an aggregate with high aspect ratio and significant persistence length.

When $K_f > K_o$ and $\sigma \ll 1$, the critical monomer concentration becomes

$$c_c = [m](\infty) = k_{off}/k_+ = K_f^{-1}. \tag{9}$$

Equation (8) is plotted with different values of K_f/K_o in Fig. 4(a). Although amyloid oligomers may grow relatively large before they nucleate into a fibrillar structure (Fig. 3), all the relevant behaviors of the system can still be captured by setting n_c=2. It appears that as the ratio K_f/K_o grows, the behavior of the system attains the characteristics of a phase transition with the free monomer concentration having a constant value irrespective of total concentration above $[m]_{tot} = c_c$ in agreement with experimental observations for amyloid systems [Fig. 4(b), Hellstrand *et al.*, 2010; Lattanzi *et al.*, 2021; and Lindberg *et al.*, 2024].

In the supplementary material, we include the opposite limit, with aggregate size is capped at two and both monomer and dimer remaining in the solution phase.

II. THERMODYNAMIC CONTROL IN A SYSTEM WITH CONSTANT TOTAL COMPOSITION

In many *in vitro* systems, the total concentration of amyloid protein monomers and all other components remain constant and known. Experiments are typically set up to start out-of-equilibrium with a surplus of monomers or fibrils. In the first case, care is taken to prepare monomers in a supersaturated state, i.e., at a concentration above their solubility limit, and the time evolution of the system or its end state is monitored (Fig. 1) (Cellmer *et al.*, 2016). The purpose of monitoring the time evolution may be to gain information on the self-assembly mechanism, in which case samples at multiple initial concentrations are typically followed, with and without a defined fraction of preformed fibrils (seeds) at time zero (Jarrett and Lansbury, 1993; Jarrett *et al.*, 1993; Cohen *et al.*, 2012; and Cohen *et al.*, 2013). The purpose of monitoring the end state may be to gain information on the solubility of the amyloid protein, in which case the experiments need to be continued until no further change is seen in the concentration of free monomers [Fig. 4(b)] (Cellmer *et al.*, 2016; Sawada *et al.*, 2020; Lattanzi *et al.*, 2021; and Lindberg *et al.*, 2024). An equilibrium state should be reachable from either end, so the same solubility should be observable upon starting from monomer-dominated and fibril-dominated samples (O'Nuallain *et al.*, 2005) (Fig. 1).

Examples of solubility investigations starting from fibril dominated samples are clear manifestations of reversibility. (Jarrett *et al.*, 1994; O'Nuallain *et al.*, 2005; Wetzel, 2006; Qiang *et al.*, 2013; and Iljina *et al.*, 2016). In these studies, fibril samples are diluted such that the free monomer concentration ends up below the solubility and a dissociation of fibrils and an increase in free monomer concentration over time is observed until equilibrium is reestablished.

Examples of solubility studies starting from monomer-dominated samples reveal how a metastable zone can be observed and can be found to shrink over a timescale of days as equilibrium is reached in more and more samples, for which the free concentration is constant

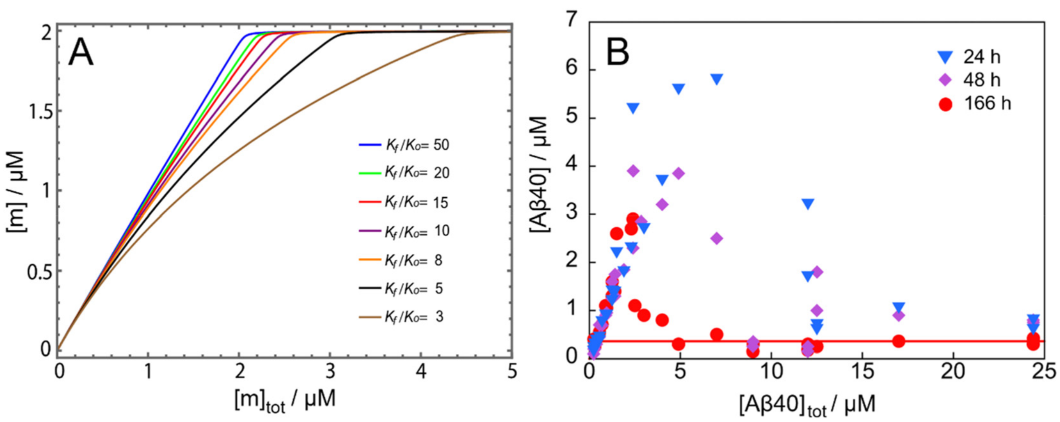

FIG. 4. Free vs total monomer concentration. (a) Numerical plot of Eq. (6) with different values of K_f/K_o. $\gamma = 0.01$, $n_c = 2$, and $K_f = 0.5\ \mu M^{-1}$. (b) Examples of experimental data for free vs total Aβ40 peptide concentration, illustrating how the system approaches equilibrium (red line) as time progresses. Data taken from Lattanzi *et al.* (2021).

irrespective of the total concentration, signifying a phase transition [Fig. 4(b); Lattanzi *et al.*, 2021; Lindberg *et al.*, 2024].

In principle, a pure system under thermodynamic control should end up in the same equilibrium state each time a reaction is setup, both in terms of the structure/morphology of the formed aggregates and the final monomer concentration. Examples of such systems are Aβ42 from AD, in which case identical ssNMR spectra were observed on multiple occasions in independently prepared samples (Colvin *et al.*, 2016).

III. KINETIC CONTROL IN A CLOSED SYSTEM

A pure system under kinetic control may end up in a state that is out of equilibrium because the energy barrier for forming the non-equilibrium state is lower or similar to the energy barrier for forming the equilibrium state (Fig. 5). A pure system under kinetic control may end up in different states each time a reaction is set up, both in terms of the structure (morphology) of the formed aggregates and the final monomer concentration (Abelein *et al.*, 2016; De Giorgi *et al.*, 2020; and Pálmadóttir *et al.*, 2023). For solutions of the α-synuclein from Parkinsons' disease, the splitting of a sample at neutral pH into multiple identical aliquots lead to initial formation of distinct samples consisting of chemically identical but morphologically different fibrils (Pálmadóttir *et al.*, 2023). The different morphologies were shown to have different solubility, different ultra-structure, and different surface properties. This was observed using NMR, CD and ThT-fluorescence spectroscopy as well as cryo-TEM. A gradual conversion from the less stable and more soluble morphology to the more stable and less soluble morphology took place over the timescale of several days. This further highlights the reversible nature of the amyloid fibrils. In this case, based on the similar frequency of initial occurrence of the two morphologies, the initial state appears to be kinetically favored due to similar nucleation barriers for the two different morphologies (Fig. 5). The end state, observed after about a week, was identified as the thermodynamically favored state (Pálmadóttir *et al.*, 2023).

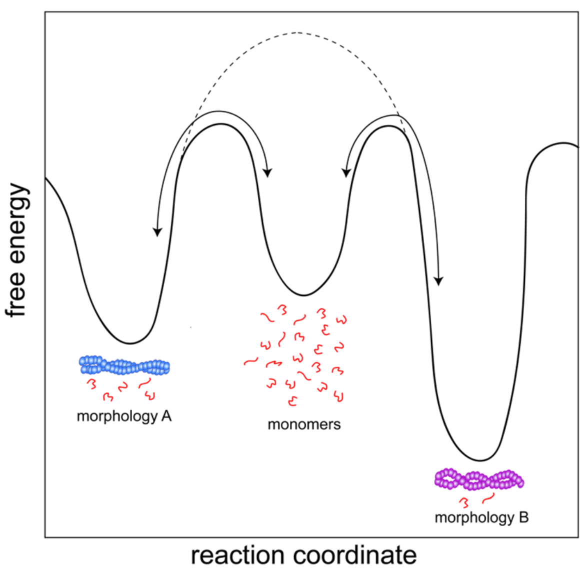

FIG. 5. Schematic illustration of the free energy landscape of two different morphologies forming at identical conditions. Fibrils of morphology A have higher solubility and are thermodynamically less stable than fibrils of morphology B, which have lower solubility (Pálmadóttir *et al.*, 2023). The free energy barriers for forming morphology A and B from monomers are of similar height, and therefore, the likelihood of forming morphology A and B is similar. As soon as a critical nucleus has been formed (or preformed fibrils added to monomeric solution), replication of the fibrils by secondary nucleation and elongation is favored over primary nucleation. A sample can, therefore, be kinetically stable, consisting of fibrils of morphology A. However, with time, the sample will always be dominated by the thermodynamically most stable fibril morphology. The formation of morphology B from a sample containing fibrils of morphology A is more likely to happen through dissociation of the less stable morphology through monomers and re-creation of the more stable morphology through nucleation and growth. Structural conversion of morphology A to B may be associated with a higher barrier (dashed lines).

Replication of the different morphologies and formation of monomorphic samples were found to be possible by adding preformed fibrils (seeds) of different morphologies to different samples. This can be explained by the energy barriers for primary nucleation being higher than the energy barriers for secondary nucleation and elongation (Cohen *et al.*, 2018), making the event of de novo nucleation less likely than the secondary nucleation and elongation of the added preformed fibrils (seeds). Primary nucleation of α-synuclein is a rare event (Campioni *et al.*, 2014; Pronchik *et al.*, 2010), and the propagation of an already existing fibril morphology is, therefore, kinetically favored (Pálmadóttir *et al.*, 2023). Despite that, at longer times, the sample will be dominated by the most stable morphology.

Similar findings have been reported for the peptide IAPP and the tau protein, in which case transient fibril morphologies were detected using cryo-EM during the amyloid formation process (Wilkinson *et al.*, 2023; Lövestam *et al.*, 2024). In both these cases, monomer dissociation and reformation of the more stable morphology through nucleation and growth may be more likely than the simultaneous structural conversion of an entire aggregate from one morphology to another (Fig. 5).

An illustrative example of this phenomenon is the observation of disappearing morphologies in crystallography. This refers to the emergence of a thermodynamically more stable crystal form, leading to the disappearance of the less stable crystal form (Bučar *et al.*, 2015). The antiviral compound Ritonavir provides an example of this phenomenon. In mid-1998, it encountered serious manufacturing problems when a new crystallized form (Form II) emerged with lower solubility. (Bauer *et al.*, 2001). Due to this new morphology, being the thermodynamically stable one, and its strong seeding capabilities, the production of the original crystal was rendered impossible in laboratories (Bučar *et al.*, 2015).

IV. PRACTICAL IRREVERSIBILITY IN CLOSED SYSTEMS DUE TO EXPERIMENTALLY INACCESSIBLE TIME SCALES

In some cases, the reverse reaction is too slow to be monitored within a practical laboratory time-frame. Studies in closed systems will fail to detect fibril dissociation upon dilution if the observation time is short relative to the inverse of the dissociation rate constant. This has led to the interpretation in some literature as the process being irreversible although a correct interpretation would rather be that the rate constant for fibril dissociation is very low. In vivo, another reason for the lack of observation of the reversibility may be the constant generation of more monomers (cf. below, Sec. VI).

When analyzing amyloid formation kinetics, it may or may not be necessary to include the reverse reaction at some or all steps. When the rate constant for monomer dissociation from fibrils is of the same order of magnitude as the inverse of the experimental time frame, it is of course necessary to include also this parameter in the analysis to faithfully evaluate the forward rate constants. However, in situations where the reverse reaction rate is orders of magnitude lower than the inverse of the experimental time frame, the forward rate constants can be reliably determined even if the back reaction is ignored. Despite the backward rate not being zero, it is difficult to observe the reversibility in situations where the net flux goes toward the build up of more and more fibrils.

As discussed earlier (Secs. I A and I C), the rate constant for monomer dissociation from fibril ends can be estimated using Eq. (1) or Eq. (9). Using published values of $S = c_c$ and k_+ for Aβ40 (in 20 mM NaP, pH 7.4, 37 °C) and Aβ42 (in 20 mM NaP, pH 8, 37 °C) (Hellstrand *et al.*, 2010; Cohen *et al.*, 2013; Meisl *et al.*, 2014; Lattanzi *et al.*, 2021; and Lindberg *et al.*, 2024), we arrive at $k_{off} = 3 \times 10^5$ $M^{-1}s^{-1} \cdot 5 \times 10^{-7}$ M $= 0.15$ s^{-1} for Aβ40 and $k_{off} = 3 \times 10^6$ $M^{-1}s^{-1} \cdot 3 \times 10^{-8}$ M $= 0.09$ s^{-1} for Aβ42. While the association rate depends on k_+, free monomer concentration, and the concentration of fibril ends, the dissociation rate depends on k_{off} and the concentration of fibril ends. Thus, if fibrils are diluted from higher to lower concentrations, the dissociation rate remains relatively constant over time because the concentration of ends decreases only slowly. This is in contrast to the case of aggregates capped at the dimer (see the supplementary material), where each dissociation event eliminates one dimer, and the dissociation rate declines more rapidly over time.

If, for example, equilibrated Aβ42 fibril sample is diluted from 5 μM to 20 nM (below S), under which condition fibrils will eventually fully dissolve, the concentration of ends will initially be on the order of 4–40 pM, assuming 1000–10 000 monomers per fibril, and the dissociation rate will be on the order of 0.4–4 pM s^{-1}. The monomer concentration after dilution will be ca. 100 pM, and the association rate will be on the order of 1–10 fM s^{-1}.

V. APPARENT REVERSIBILITY UPON SYSTEM CHANGE

The reversibility of amyloid formation is apparent under system change, for example, when the temperature (Löwik *et al.*, 2005; van den Heuvel *et al.*, 2008; Arora *et al.*, 2004; Morel *et al.*, 2010; Kardos *et al.*, 2011; Ikenoue *et al.*, 2014; Sudhakar and Mani, 2019; Norrild *et al.*, 2021; Takeda and Klimov, 2008; and Andrýsková *et al.*, 2023), pH (Fig. 6) (Tipping *et al.*, 2015; Shammas *et al.*, 2011; Shimanovich *et al.*, 2021; and Röder *et al.*, 2019), ionic strength (Raman *et al.*, 2005; Abelein *et al.*, 2016; and Shukla *et al.*, 2017), pressure (Foguel *et al.*, 2003; Torrent *et al.*, 2006; and Rezaei-Ghaleh *et al.*, 2016), denaturant concentration (Narimoto *et al.*, 2004; Sneideris *et al.*, 2015; Sil *et al.*, 2018; Vettore and Buell, 2019; and Farzadfard *et al.*, 2024) or solvent (Hirota-Nakaoka *et al.*, 2003) is altered, or upon the addition of chaperones (Parsell *et al.*, 1994; Glover and Lindquist, 1998; Shorter, 2011; Nillegoda *et al.*, 2015; Gao *et al.*, 2015; Ferrari *et al.*, 2018; Kannaian *et al.*, 2019; and Wentink *et al.*, 2020). If the most stable morphology is not altered due to the system change, this is a convenient way to manifest and quantify thermodynamic reversibility. Fibril formation reactions are typically studied after a temperature jump from for example 0 to 37 °C, and conversely the higher solubility at lower and higher temperatures allows the backward reaction to be studied upon cooling or heating (Kardos *et al.*, 2011; Ikenoue *et al.*, 2014; and Norrild *et al.*, 2021). Pressure changes is another convenient way to promote or reverse amyloid fibril formation (Foguel *et al.*, 2003; Torrent *et al.*, 2006).

Conditions may change so much that the initial fibril structure becomes unstable and another structure is governed. Such more drastic perturbations of the environment may allow for easy experimental observation of amyloid fibril dissociation. For example, when a fibril structure is governed by disulfide bonds, their reduction may lead to

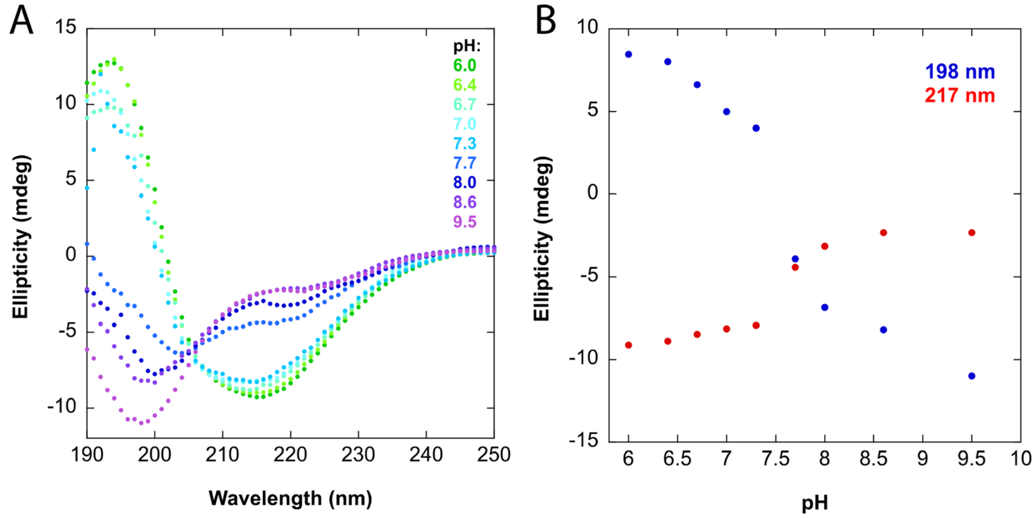

FIG. 6. Dissolution of α-synuclein fibrils upon pH change. (a) Fibrils were formed at pH 6 (20 μM α-synuclein, 10 mM MES, 1% seeds, pH 6.0) and titrated with 1M NaOH and changes in secondary structure were monitored by recording circular dichroism spectra. At the lower pH values (6–6.7), the sample showed β-sheet structure, confirming the presence of amyloid fibrils. At pH 7.3, the structure started dissolving into random coil, indicating dissociation of the fibrils into monomers (b) The intensity at 198 and 217 nm vs pH. The time between pH change and CD measurement is within minutes. These results imply the importance of exploring the pH stability of the amyloid structures of interest, to study dissociation upon pH change.

fibril dissociation (Heath *et al.*, 2024). A striking example is provided by α-synuclein, the fibril structure of which is highly dependent on solution conditions (Gath *et al.*, 2014; Bousset *et al.*, 2023). For this protein, changes in, for example, pH leads to rapid dissociation of fibrils to establish a new equilibrium as exemplified in Fig. 6.

The human lysozyme and its homolog from hen egg white are examples of proteins that have been found to form different amyloid fibril morphologies, depending on the folding path. The different morphologies showed different heat tolerance and either dissolved, showing clear signs of reversibility upon system change or did not dissolve (Cao *et al.*, 2021). This highlights that the apparent reversibility is highly dependent on the solution conditions, which may change the heights of the kinetic barriers for fibril formation and dissolution. Different folds will naturally possess individual stabilities and barriers and be differentially susceptible to dissolution and, thus, may or may not display reversibility over a practical laboratory time frame.

VI. PRACTICAL IRREVERSIBILITY IN SYSTEMS WITH CONTINUOUS MONOMER PRODUCTION

While the systems described above provide fundamental insight into the amyloid formation process and its reversibility, a very different situation arises in amyloid diseases where monomers are continuously being produced and added to the system after the first aggregates deposits have precipitated. Proteostasis *in vivo* keeps proteins at a relatively constant (and often low) monomer concentration. Thus, after the emergence of the first aggregates, the amount of precipitated aggregates may be continuously growing while the monomer concentration remains relatively constant. An amyloid disease may in such situation be viewed as having reached a state of no return, which may be tempting to interpret as the underlying process being irreversible. However, even if the systemic effect may be practically irreversible, both monomer addition and monomer dissociation continue all the time in a reversible manner, and the underlying process is reversible even if the microscopic rates are not balanced in this situation. Under continuous production of monomers, the fibrils will never dissociate, and the system may be practically viewed as in an irreversible state although it is more correctly viewed as constantly out of equilibrium and drifting toward more and more precipitated monomers. One way to model such a situation is to add a source term to the kinetic equation (Wei *et al.*, 2024). Additionally, in living systems, amyloid aggregate clearance processes are also present but may not balance the production, which adds complexity to the kinetics of amyloid aggregation (Dear *et al.*, 2024).

VII. PRACTICAL IRREVERSIBILITY IN SYSTEMS WITH MONOMER CHEMICAL MODIFICATIONS

Yet, another situation arises in amyloid systems where monomers are chemically modified after fibril formation, e.g., through chemical cross-linking (Al-Hilaly *et al.*, 2013; Wördehoff *et al.*, 2017), oxidation (Binger *et al.*, 2008), phosphorylation (Anderson *et al.*, 2006; Rezaei-Ghaleh *et al.*, 2016), ubiquitination (Hasegawa *et al.*, 2002; Anderson *et al.*, 2006), deamidation (Nilsson and Dobson, 2003), as well as through degradation or truncation of monomers (Anderson *et al.*, 2006; Ariesandi *et al.*, 2013; and Ortigosa-Pascual *et al.*, 2023). For example, high temperature treatments of α-synuclein have been found to result in truncation within the C-terminal tail, at Asp119 (Ariesandi *et al.*, 2013). Truncation at the same position has also been observed at physiological temperatures *in vitro*, after prolonged incubation time as well as in connection with fibril formation (Ortigosa-Pascual *et al.*, 2023). Variant dimer bands were detected at the end of an aggregation reaction and only in the fractions containing fibrils that had been separated from monomers through centrifugation (Ortigosa-Pascual *et al.*, 2023). The Asp 119 truncation has also been detected *in vivo* (Anderson *et al.*, 2006). Such modifications could possibly result in other morphologies being more favorable, and thus, affect the stability as well as the reversibility relative to the initial structure. Additionally, dityrosine cross-linking of α-synuclein fibrils has been shown to stabilize their structure and increase their resistance to chemical denaturation (Wördehoff *et al.*, 2017). Another example is the formation of cross-linked Aβ dimers (Brinkmalm *et al.*, 2019; Al-Hilaly *et al.*, 2013), which may affect the fibril dissociation rate.

VIII. REGULATION OF FUNCTIONAL AMYLOIDS IN *IN VIVO* SYSTEMS BY ENVIRONMENTAL CHANGES

In addition to pathological amyloids, there are functional amyloids that have various biological roles (Maji *et al.*, 2009; Otzen and Riek, 2019; Ke *et al.*, 2020). Functional amyloids are an example of how nature has taken advantage of the amyloid structure and its reversibility, with growth and dissociation regulated by various factors, such as temperature, pH, nutrient availability, and developmental stage of the organism (Nespovitaya *et al.*, 2016; Dharmadana *et al.*, 2019; McGlinchey and Lee, 2017; Saad *et al.*, 2017; Cereghetti *et al.*, 2018; Liu *et al.*, 2021; and Cereghetti *et al.*, 2024). One example is the developmentally regulated co-aggregation of the RNA-binding protein Rim4 and mRNA during meiosis stage I in yeast. At the onset of meiosis stage II, these aggregates disassemble, allowing mRNA translation to resume and thereby promoting and facilitating the cell cycle progression (Cereghetti *et al.*, 2018). Another example is the reversible fibril formation of peptide hormones, such as, e.g., β-endorphin and gonadotropin-releasing hormone, which is highly dependent on environmental factors, such as pH and polyprotic acids. (Liu *et al.*, 2021; Nespovitaya *et al.*, 2016; and Dharmadana *et al.*, 2019). Another example is the aggregation of the yeast pyruvate kinase Cdc19 upon glucose starvation and heat shock. This is a highly regulated preventive mechanism against stress, where the aggregates dissolve within minutes upon the addition of glucose (Saad *et al.*, 2017). It has been shown that both the yeast and the human pyruvate kinase have a pH sensitive core resulting in either amyloid formation or dissociation depending on the pH changes (Cereghetti *et al.*, 2024). The pH regulated disaggregation of the repeat domains of the functional amyloid Pmel17, involved in melanin biosynthesis is yet another example of reversibility of a functional amyloid (McGlinchey and Lee, 2017). Studies of functional amyloids have indicated that the presence of low complexity regions (LCRs) containing phosphorylation sites might be crucial for the regulation of the reversibility (Saad *et al.*, 2017; Cereghetti *et al.*, 2018).

IX. REVERSIBILITY OF SYNTHETIC PEPTIDES

The development of solid-phase peptide synthesis (Merrifield, 1963; Howl, 2005) paved the way for systematic studies of short (of the order of ten residues) peptides' self-assembly (Zhang, 2017). An area that has grown extensively in recent years. Most work in this area has concerned peptide based materials science (Fairman and Åkerfeldt, 2005; Gazit, 2007; Ulijn and Smith, 2008; and Guler, 2021), typically for various biomedical applications (Matson *et al.*, 2011; Sun *et al.*, 2016; and Fichman *et al.*, 2021), but there has also been studies on the thermodynamics and kinetics of peptide self-assembly (Nyrkova *et al.*, 2000; Semenov and Subbotin, 2010; Rüter *et al.*, 2019; and Rüter *et al.*, 2020). Within the aim to understand protein amyloid formation and the properties of amyloid fibrils, one may possibly learn from these studies of short synthetic peptides. The most common morphology of short peptide assemblies are, in fact, long fibrils, with intermolecular β-sheets in the fibril direction, thus sharing similarities with amyloid fibrils. As for the amyloid proteins, the driving force for self-assembly of short peptides is dominated by hydrophobic interactions. With designed synthesis, the hydrophobic peptide–peptide interactions can be tuned in a controlled way and systematically investigated. For example, monomer solubility can be tuned to be in the mM range, where it can be accurately measured by simple light scattering experiment (Çenker *et al.*, 2014), and where aggregation (Çenker *et al.*, 2012) and dissolution (Koder Hamid *et al.*, 2020) kinetics are easily investigated, allowing for an easy and clear demonstration of that pepide self-assembly being reversible.

X. UTILIZING AMYLOID FIBRIL REVERSIBILITY FOR FUNCTIONAL BIOMATERIALS

The understanding of the formation of amyloid fibrils and their unique properties has already served as a foundation for the design of different biomaterials (Cherny and Gazit, 2008; Romero *et al.*, 2010; Wei *et al.*, 2017; Knowles and Buehler, 2011; and Jacob *et al.*, 2019) and for development within the field of drug delivery (Ping *et al.*, 2017). Increased knowledge of the reversibility of the amyloid structures can further enhance the innovative design process (Wang *et al.*, 2016). The fact that charged fibrils readily form hydrogels may be utilized within materials science, nanotechnology, and drug delivery, where the reversibility would serve as the key for tuning a system and/or changing the materials' properties (e.g., forming or dissolving the fibrils and the hydrogel) upon systems change. This phenomenon has been found within a system containing the Sg38-48 peptide, named the KD peptide, which self-assembles into amyloid fibrils and dissociates back to its monomeric form as a function of pH (Shimanovich *et al.*, 2021). Oat globulin from the oat plant has been found to form reversible amyloid fibrils that can be used for water membranes, electrodes, aerogels, and sensors (Zhou *et al.*, 2022). The reversibility of amyloid structures could also be important within the field of drug delivery. Studies of gonadotropin-releasing hormone analogs have shown that the monomer-fibril equilibrium (reversibility) can be leveraged for the development of long-acting drugs (Maji *et al.*, 2008).

Reversibility also provides a healing process ensuring that the most stable assembly forms more quickly. On average, "correctly associated" monomers will display slower dissociation than "wrongly associated" ones. Thus, monomers that have not adopted the more stable fold and nearest-neighbor contacts of the final assembly will dissociate quickly allowing for new monomers to associate in a more productive manner.

XI. REVERSIBILITY IN AMYLOID DISORDERS IN VIVO

Many protein misfolding disease are characterized by the aberrant deposition in different parts of the body of proteins with apparently higher solubility in the healthy state. Notably, this is the case for Alzheimer's disease, which is driven by amyloid aggregation of the Aβ peptide in the extracellular space in the central nervous system and the tau protein in the intracellular space; and Parkinson's disease which is associated with the aggregation of α-synuclein. It has become increasingly clear that a gain of dysfunction (toxicity) from the aggregated form of the proteins is a key driver of the disease and, thus, significant efforts have focused on therapeutic strategies which can reduce the aggregate burden. Therapeutics may harness the key feature of amyloid formation as a reversible process to shift the equilibrium through solubilization or clearance (Figs. 1 and 7).

Such therapeutics include the antibodies aducanumab (Sevigny *et al.*, 2016), lecanemab (van Dyck *et al.*, 2023), and donanemab (Sims *et al.*, 2023), which bind to aggregated forms of Aβ, and which increase the clearance of amyloid plaques in Alzheimer's disease. A concern with clearance-based therapies that do not simply promote monomer dissociation may be the increased appearance of toxic oligomeric species. Another mechanism of therapeutics involves the stabilization of the protein species in solution. The small molecule tafamidis is an example of an established therapeutic molecule, which is found to stabilize the transthyretin tetramer in the solution phase (Coelho *et al.*, 2016), thus driving the reversible amyloid system away from the fibrillar state and lowering the risk of transthyretin amyloidosis.

A particularly interesting recent set of approaches have focused on reducing the production of the aggregating protein, for instance, tau (Vemula *et al.*, 2023). Remarkably, clinical data have shown that simply inhibiting the production of the monomeric protein is enough to reverse the amyloid assembly process, and significantly decreased aggregate loads have been demonstrated in patients treated with such modalities. Although different active clearance mechanisms are likely to contribute to this disassembly reaction, it is likely that the simple

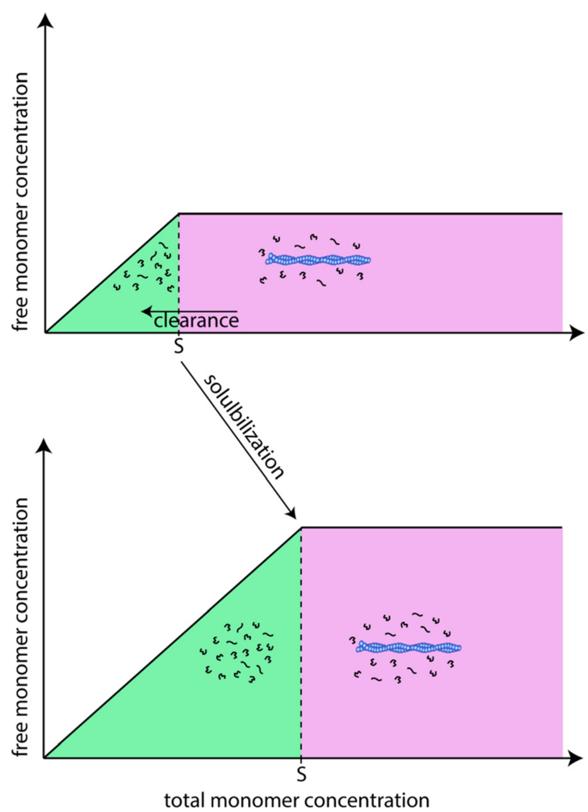

FIG. 7. Therapeutic strategies. Clearance (top) or solubilization (bottom) are two potential therapeutic routes based on the reversible nature of amyloid formation.

reversibility discussed in this review can lead to the reversal of the assembly process once the monomer concentration decreases below the critical concentration.

XII. CONCLUSIONS

Amyloid formation is a non-covalent assembly process, and its reversibility is well documented by experimental studies, as exemplified in the current perspective. As reviewed, the reversibility can be observed upon dilution of fibrils under otherwise constant solution conditions or under changes in the solution conditions that increases the solubility of the amyloid system at hand. The dissociation may, however, be so slow that the process can be viewed as practically irreversible over a given time frame or because the system at hand contains a source for constant monomer addition, leading to net buildup of amyloid even if both growth and dissociation occur at all times. Reversibility is also a key to the performance of fibril-based biomaterials and functional amyloid.

SUPPLEMENTARY MATERIAL

See the supplementary material for the modeling of reversible amyloid formation.

ACKNOWLEDGMENTS

The current work was supported by grants from the Swedish Research Council (No. VR 2015-00143), the European Research Council (No. 101097824), and the Knut and Alice Wallenberg Foundation (No. 2022.0059).

AUTHOR DECLARATIONS

Conflict of Interest

The authors have no conflicts to disclose.

Author Contributions

Tinna Pálmadóttir: Investigation (equal); Visualization (equal); Writing – original draft (equal); Writing – review & editing (lead). **Josef Getachew:** Investigation (equal); Visualization (equal); Writing – review & editing (equal). **Lei Ortigosa-Pascual:** Investigation (equal); Visualization (equal); Writing – review & editing (equal). **Emil Axell:** Writing – review & editing (equal). **Jiapeng Wei:** Investigation (equal); Visualization (equal); Writing – review & editing (equal). **Ulf Olsson:** Investigation (equal); Visualization (equal); Writing – review & editing (equal). **Tuomas P. J. Knowles:** Conceptualization (equal); Investigation (equal); Visualization (equal); Writing – review & editing (equal). **Sara Linse:** Conceptualization (equal); Investigation (equal); Visualization (equal); Writing – original draft (equal); Writing – review & editing (equal).

DATA AVAILABILITY

The data that support the findings of this study are available from the corresponding authors upon reasonable request.

REFERENCES

Abelein, A., Jarvet, J., Barth, A., Gräslund, A., and Danielsson, J., "Ionic strength modulation of the free energy landscape of Aβ_{40} peptide fibril formation," J. Am. Chem. Soc. **138**(21), 6893–6902 (2016).

Adamcik, J. and Mezzenga, R., "Amyloid polymorphism in the protein folding and aggregation energy landscape," Angew. Chem., Int. Ed. **57**(28), 8370–8382 (2018).

Al-Hilaly, Y. K., Williams, T. L., Stewart-Parker, M., Ford, L., Skaria, E., Cole, M., Bucher, W. G., Morris, K. L., Sada, A. A., Thorpe, J. R., and Serpell, L. C., "A central role for dityrosine crosslinking of Amyloid-β in Alzheimer's disease," Acta Neuropathol. Commun. **1**, 83 (2013).

Anderson, J. P., Walker, D. E., Goldstein, J. M., de Laat, R., Banducci, K., Caccavello, R. J., Barbour, R., Huang, J., Kling, K., Lee, M., Diep, L., Keim, P. S., Shen, X., Chataway, T., Schlossmacher, M. G., Seubert, P., Schenk, D., Sinha, S., Gai, W. P., and Chilcote, T. J., "Phosphorylation of Ser-129 is the dominant pathological modification of alpha-synuclein in familial and sporadic Lewy body disease," J. Biol. Chem. **281**(40), 29739–29752 (2006).

Andrýsková, N., Vrbovská, H., Babincová, M., Babinec, P., and Simaljaková, M., "Dissolution of lysozyme amyloid fibrils using magnetic nanoparticles in an alternating magnetic field: Design of an effective treatment for cutaneous amyloidosis," Magnetochemistry **9**(3), 84 (2023).

Ariesandi, W., Chang, C. F., Chen, T. E., and Chen, Y. R., "Temperature-dependent structural changes of Parkinson's alpha-synuclein reveal the role of pre-existing oligomers in alpha-synuclein fibrillization," PLoS One **8**(1), e53487 (2013).

Arora, A., Ha, C., and Park, C. B., "Insulin amyloid fibrillation at above 100 °C: New insights into protein folding under extreme temperatures," Protein Sci. **13**(9), 2429–2436 (2004).

Arosio, P., Cukalevski, R., Frohm, B., Knowles, T. P., and Linse, S., "Quantification of the concentration of Aβ42 propagons during the lag phase by an amyloid chain reaction assay," J. Am. Chem. Soc. **136**(1), 219–225 (2014).

Arosio, P., Knowles, T. P., and Linse, S., "On the lag phase in amyloid fibril formation," Phys. Chem. Chem. Phys. **17**(12), 7606–7618 (2015).

Balchin, D., Hayer-Hartl, M., and Hartl, F. U., "In vivo aspects of protein folding and quality control," Science **353**(6294), aac4354 (2016).

Bauer, J., Spanton, S., Henry, R., Quick, J., Dziki, W., Porter, W., and Morris, J., "Ritonavir: An extraordinary example of conformational polymorphism," Pharm. Res. **18**, 859–866 (2001).

Binger, K. J., Griffin, M. D., and Howlett, G. J., "Methionine oxidation inhibits assembly and promotes disassembly of apolipoprotein C-II amyloid fibrils," Biochemistry **47**(38), 10208–10217 (2008).

Bousset, L., Alik, A., Arteni, A., Böckmann, A., Meier, B. H., and Melki, R., "α-Synuclein Fibril, Ribbon and Fibril-91 Amyloid polymorphs generation for structural studies," Methods Mol. Biol. **2551**, 345–355 (2023).

Brinkmalm, G., Hong, W., Wang, Z., Liu, W., O'Malley, T. T., Sun, X., Frosch, M. P., Selkoe, D. J., Portelius, E., Zetterberg, H., Blennow, K., and Walsh, D. M., "Identification of neurotoxic cross-linked amyloid-β dimers in the Alzheimer's brain," Brain **142**(5), 1441–1457 (2019).

Brännström, K., Islam, T., Gharibyan, A. L., Iakovleva, I., Nilsson, L., Lee, C. C., Sandblad, L., Pamrén, A., and Olofsson, A., "The properties of amyloid-β fibrils are determined by their path of formation," J. Mol. Biol. **430**(13), 1940–1949 (2018).

Bučar, D. K., Lancaster, R. W., and Bernstein, J., "Disappearing polymorphs revisited," Angew. Chem., Int. Ed. **54**(24), 6972–6993 (2015).

Buell, A. K., "The growth of amyloid fibrils: Rates and mechanisms," Biochem. J. **476**(19), 2677–2703 (2019).

Buell, A. K., Dobson, C. M., and Welland, M. E., "Measuring the kinetics of amyloid fibril elongation using quartz crystal microbalances," Methods Mol. Biol. **849**, 101–119 (2012).

Buell, A. K., Galvagnion, C., Gaspar, R., Sparr, E., Vendruscolo, M., Knowles, T. P., Linse, S., and Dobson, C. M., "Solution conditions determine the relative importance of nucleation and growth processes in α-synuclein aggregation," Proc. Natl. Acad. Sci. U. S. A. **111**(21), 7671–7676 (2014).

Buell, A. K., "Stability matters, too - the thermodynamics of amyloid fibril formation," Chem. Sci. **13**(35), 10177–10192 (2022).

Campioni, S., Carret, G., Jordens, S., Nicoud, L., Mezzenga, R., and Riek, R., "The presence of an air-water interface affects formation and elongation of α-Synuclein fibrils," J. Am. Chem. Soc. **136**(7), 2866–2875 (2014).

Cao, Y., Adamcik, J., Diener, M., Kumita, J. R., and Mezzenga, R., "Different folding states from the same protein sequence determine reversible vs irreversible amyloid fate," J. Am. Chem. Soc. **143**(30), 11473–11481 (2021).

Cellmer, T., Ferrone, F. A., and Eaton, W. A., "Universality of supersaturation in protein-fiber formation," Nat. Struct. Mol. Biol. **23**(5), 459–461 (2016).
Çenker, C. Ç., Bucak, S., and Olsson, U., "Aqueous self-assembly within the homologous peptide series AnK," Langmuir **30**(33), 10072–10079 (2014).
Çenker, Ç. Ç., Bomans, P. H. H., Friedrich, H., Dedeoglu, B., Aviyente, V., Olsson, U., Sommerdijk, N. A. J. M., and Bucak, S., "Peptide nanotube formation: A crystal growth process," Soft Matter **8**, 7463–7470 (2012).
Cereghetti, G., Saad, S., Dechant, R., and Peter, M., "Reversible, functional amyloids: Towards an understanding of their regulation in yeast and humans," Cell Cycle **17**(13), 1545–1558 (2018).
Cereghetti, G., Kissling, V. M., Koch, L. M., Arm, A., Schmidt, C. C., Thüringer, Y., Zamboni, N., Afanasyev, P., Linsenmeier, M., Eichmann, C., Kroschwald, S., Zhou, J., Cao, Y., Pfizenmaier, D. M., Wiegand, T., Cadalbert, R., Gupta, G., Boehringer, D., Knowles, T. P. J., Mezzenga, R., Arosio, P., Riek, R., and Peter, M., "An evolutionary conserved mechanism controls reversible amyloids of pyruvate kinase via pH-sensing regions," Dev. Cell **59**(14), 1876–1891.e7 (2024).
Cherny, I. and Gazit, E., "Amyloids: Not only pathological agents but also ordered nanomaterials," Angew. Chem., Int. Ed. **47**(22), 4062–4069 (2008).
Chiti, F. and Dobson, C. M., "Protein misfolding, functional amyloid, and human disease," Annu. Rev. Biochem. **75**, 333–366 (2006).
Chiti, F. and Dobson, C. M., "Protein misfolding, amyloid formation, and human disease: A summary of progress over the last decade," Annu. Rev. Biochem. **86**, 27–68 (2017).
Coelho, T., Merlini, G., Bulawa, C. E., Fleming, J. A., Judge, D. P., Kelly, J. W., Maurer, M. S., Planté-Bordeneuve, V., Labaudinière, R., Mundayat, R., Riley, S., Lombardo, I., and Huertas, P., "Mechanism of action and clinical application of tafamidis in hereditary transthyretin amyloidosis," Neurol. Ther. **5**(1), 1–25 (2016).
Cohen, S. I., Vendruscolo, M., Dobson, C. M., and Knowles, T. P., "From macroscopic measurements to microscopic mechanisms of protein aggregation," J. Mol. Biol. **421**(2–3), 160–171 (2012).
Cohen, S. I., Linse, S., Luheshi, L. M., Hellstrand, E., White, D. A., Rajah, L., Otzen, D. E., Vendruscolo, M., Dobson, C. M., and Knowles, T. P., "Proliferation of amyloid-β42 aggregates occurs through a secondary nucleation mechanism," Proc. Natl. Acad. Sci. U. S. A. **110**(24), 9758–9763 (2013).
Cohen, S. I. A., Cukalevski, R., Michaels, T. C. T., Šarić, A., Törnquist, M., Vendruscolo, M., Dobson, C. M., Buell, A. K., Knowles, T. P. J., and Linse, S., "Distinct thermodynamic signatures of oligomer generation in the aggregation of the amyloid-β peptide," Nat. Chem. **10**(5), 523–531 (2018).
Colvin, M. T., Silvers, R., Ni, Q. Z., Can, T. V., Sergeyev, I., Rosay, M., Donovan, K. J., Michael, B., Wall, J., Linse, S., and Griffin, R. G., "Atomic resolution structure of monomorphic Aβ42 amyloid fibrils," J. Am. Chem. Soc. **138**(30), 9663–9674 (2016).
Comas-Garcia, M., Garmann, R. F., Singaram, S. W., Ben-Shaul, A., Knobler, C. M., and Gelbart, W. M., "Characterization of viral capsid protein self-assembly around short single-stranded RNA," J. Phys. Chem. B **118**(27), 7510–7519 (2014).
De Giorgi, F., Laferrière, F., Zinghirino, F., Faggiani, E., Lends, A., Bertoni, M., Yu, X., Grélard, A., Morvan, E., Habenstein, B., Dutheil, N., Doudnikoff, E., Daniel, J., Claverol, S., Qin, C., Loquet, A., Bezard, E., and Ichas, F., "Novel self-replicating α-synuclein polymorphs that escape ThT monitoring can spontaneously emerge and acutely spread in neurons," Sci. Adv. **6**(40), eabc4364 (2020).
Dear, A. J., Meisl, G., Šarić, A., Michaels, T. C. T., Kjaergaard, M., Linse, S., and Knowles, T. P. J., "Identification of on- and off-pathway oligomers in amyloid fibril formation," Chem. Sci. **11**(24), 6236–6247 (2020).
Dear, A. J., Thacker, D., Wennmalm, S., Ortigosa-Pascual, L., Andrzejewska, E. A., Meisl, G., Linse, S., and Knowles, T. P. J., "Aβ oligomer dissociation is catalyzed by fibril surfaces," ACS Chem. Neurosci. **15**(11), 2296–2307 (2024).
Dharmadana, D., Reynolds, N. P., Conn, C. E., and Valéry, C., "pH-dependent self-assembly of human neuropeptide hormone GnRH into functional amyloid nanofibrils and hexagonal phases," ACS Appl. Bio Mater. **2**(8), 3601–3606 (2019).
Eanes, E. D. and Glenner, G. G., "X-ray diffraction studies on amyloid filaments," J. Histochem. Cytochem. **16**(11), 673–677 (1968).
Evans, D. F. and Wennerström, H., *The Colloidal Domain* (Wiley-VCH, 1999).
Eves, B. J., Doutch, J. J., Terry, A. E., Yin, H., Moulin, M., Haertlein, M., Forsyth, V. T., Flagmeier, P., Knowles, T. P. J., Dias, D. M., Lotze, G., Seddon, A. M., and Squires, A. M., "Elongation rate and average length of amyloid fibrils in solution using isotope-labelled small-angle neutron scattering," RSC Chem. Biol. **2**(4), 1232–1238 (2021).
Fairman, R. and Åkerfeldt, K. S., "Peptides as novel smart materials," Curr. Opin. Struct. Biol. **15**(4), 453–463 (2005).
Farzadfard, A., Kunka, A., Mason, T. O., Larsen, J. A., Norrild, R. K., Dominguez, E. T., Ray, S., and Buell, A. K., "Thermodynamic characterization of amyloid polymorphism by microfluidic transient incomplete separation," Chem. Sci. **15**(7), 2528–2544 (2024).
Fichman, G., Andrews, C., Patel, N. L., and Schneider, J. P., "Antibacterial gel coatings inspired by the cryptic function of a mussel Byssal peptide," Adv. Mater. **33**(40), e2103677 (2021).
Ferrari, L., Geerts, W. J. C., van Wezel, M., Kos, R., Konstantoulea, A., van Bezouwen, L. S., Förster, F. G., and Rüdiger, S. G. D., "Human chaperones untangle fibrils of the Alzheimer protein Tau," bioRxiv (2018).
Foderà, V., Librizzi, F., Groenning, M., van de Weert, M., and Leone, M., "Secondary nucleation and accessible surface in insulin amyloid fibril formation," J. Phys. Chem. B **112**(12), 3853–3858 (2008).
Foguel, D., Suarez, M. C., Ferrão-Gonzales, A. D., Porto, T. C., Palmieri, L., Einsiedler, C. M., Andrade, L. R., Lashuel, H. A., Lansbury, P. T., Kelly, J. W., and Silva, J. L., "Dissociation of amyloid fibrils of alpha-synuclein and transthyretin by pressure reveals their reversible nature and the formation of water-excluded cavities," Proc. Natl. Acad. Sci. U. S. A. **100**(17), 9831–9836 (2003).
Frackowiak, J., Zoltowska, A., and Wisniewski, H. M., "Non-fibrillar beta-amyloid protein is associated with smooth muscle cells of vessel walls in Alzheimer disease," J. Neuropathol. Exp. Neurol. **53**(6), 637–645 (1994).
Frey, L., Zhou, J., Cereghetti, G., Weber, M. E., Rhyner, D., Pokharna, A., Wenchel, L., Kadavath, H., Cao, Y., Meier, B. H., Peter, M., Greenwald, J., Riek, R., and Mezzenga, R., "A structural rationale for reversible vs irreversible amyloid fibril formation from a single protein," Nat. Commun. **15**(1), 8448 (2024).
Gao, X., Carroni, M., Nussbaum-Krammer, C., Mogk, A., Nillegoda, N. B., Szlachcic, A., Guilbride, D. L., Saibil, H. R., Mayer, M. P., and Bukau, B., "Human Hsp70 disaggregase reverses Parkinson's-linked α-synuclein amyloid fibrils," Mol. Cell **59**(5), 781–793 (2015).
Gaspar, R., Meisl, G., Buell, A. K., Young, L., Kaminski, C. F., Knowles, T. P. J., Sparr, E., and Linse, S., "Secondary nucleation of monomers on fibril surface dominates α-synuclein aggregation and provides autocatalytic amyloid amplification," Q. Rev. Biophys. **50**, e6 (2017).
Gath, J., Bousset, L., Habenstein, B., Melki, R., Böckmann, A., and Meier, B. H., "Unlike twins: An NMR comparison of two alpha-synuclein polymorphs featuring different toxicity," PLoS One **9**(3), e90659 (2014).
Gazit, E., "Self-assembled peptide nanostructures: The design of molecular building blocks and their technological utilization," Chem. Soc. Rev. **36**, 1263–1269 (2007).
Glover, J. R. and Lindquist, S., "Hsp104, Hsp70, and Hsp40: A novel chaperone system that rescues previously aggregated proteins," Cell **94**(1), 73–82 (1998).
Goto, Y., Nakajima, K., Yamamoto, S., and Yamaguchi, K., "Supersaturation, a critical factor underlying proteostasis of amyloid fibril formation," J. Mol. Biol. **436**, 168475 (2024).
Guler, M. O., *Peptide-Based Biomaterials* (The Royal Society of Chemistry, 2021).
Hasegawa, M., Fujiwara, H., Nonaka, T., Wakabayashi, K., Takahashi, H., Lee, V. M., Trojanowski, J. Q., Mann, D., and Iwatsubo, T., "Phosphorylated alpha-synuclein is ubiquitinated in alpha-synucleinopathy lesions," J. Biol. Chem. **277**(50), 49071–49076 (2002).
Heath, S. G., Gray, S. G., Hamzah, E. M., O'Connor, K. M., Bozonet, S. M., Botha, A. D., de Cordovez, P., Magon, N. J., Naughton, J. D., Goldsmith, D. L. W., Schwartfeger, A. J., Sunde, M., Buell, A. K., Morris, V. K., and Göbl, C., "Amyloid formation and depolymerization of tumor suppressor p16$^{\mathrm{INK4a}}$ are regulated by a thiol-dependent redox mechanism," Nat. Commun. **15**(1), 5535 (2024).
Hellstrand, E., Boland, B., Walsh, D. M., and Linse, S., "Amyloid β-protein aggregation produces highly reproducible kinetic data and occurs by a two-phase process," ACS Chem. Neurosci. **1**(1), 13–18 (2010).

Hirota-Nakaoka, N., Hasegawa, K., Naiki, H., and Goto, Y., "Dissolution of β_2-microglobulin amyloid fibrils by dimethylsulfoxide," J. Biochem. **134**(1), 159–164 (2003).

Howl, J., *Peptide Synthesis and Applications* (Humana Press, Totawa, NJ, 2005).

Iadanza, M. G., Jackson, M. P., Hewitt, E. W., Ranson, N. A., and Radford, S. E., "A new era for understanding amyloid structures and disease," Nat. Rev. Mol. Cell Biol. **19**(12), 755–773 (2018).

Ikenoue, T., Lee, Y. H., Kardos, J., Saiki, M., Yagi, H., Kawata, Y., and Goto, Y., "Cold denaturation of alpha-synuclein amyloid fibrils," Angew. Chem., Int. Ed. **53**(30), 7799–7804 (2014).

Iljina, M., Garcia, G. A., Dear, A. J., Flint, J., Narayan, P., Michaels, T. C., Dobson, C. M., Frenkel, D., Knowles, T. P., and Klenerman, D., "Quantitative analysis of co-oligomer formation by amyloid-β peptide isoforms," Sci. Rep. **6**, 28658 (2016).

Jacob, R. S., Anoop, A., and Maji, S. K., "Protein nanofibrils as storage forms of peptide drugs and hormones," Adv. Exp. Med. Biol. **1174**, 265–290 (2019).

Jahn, T. R., Makin, O. S., Morris, K. L., Marshall, K. E., Tian, P., Sikorski, P., and Serpell, L. C., "The common architecture of cross-β amyloid," J. Mol. Biol. **395**(4), 717–727 (2010).

Jarrett, J. T., Berger, E. P., and Lansbury, P. T., Jr., "The carboxy terminus of the β amyloid protein is critical for the seeding of amyloid formation: Implications for the pathogenesis of Alzheimer's disease," Biochemistry **32**, 4693–4697 (1993).

Jarrett, J. T. and Lansbury, P. T., Jr., "Seeding "one-dimensional crystallization" of amyloid: A pathogenic mechanism in Alzheimer's disease and scrapie?" Cell **73**(6), 1055–1058 (1993).

Jarrett, J. T., Costa, P. R., Griffin, R. G., and Lansbury, P. T., Jr., "Models of the β protein C-terminus: Differences in Amyloid structure may lead to segregation of "long" and "short" fibrils," J. Am. Chem. Soc. **116**, 9741–9742 (1994).

Kardos, J., Yamamoto, K., Hasegawa, K., Naiki, H., and Goto, Y., "Direct measurement of the thermodynamic parameters of amyloid formation by isothermal titration calorimetry," J. Biol. Chem. **279**(53), 55308–55314 (2004).

Kardos, J., Micsonai, A., Pál-Gábor, H., Petrik, É., Gráf, L., Kovács, J., Lee, Y. H., Naiki, H., and Goto, Y., "Reversible heat-induced dissociation of β_2-microglobulin amyloid fibrils," Biochemistry **50**(15), 3211–3220 (2011).

Ke, P. C., Zhou, R., Serpell, L. C., Riek, R., Knowles, T. P. J., Lashuel, H. A., Gazit, E., Hamley, I. W., Davis, T. P., Fändrich, M., Otzen, D. E., Chapman, M. R., Dobson, C. M., Eisenberg, D. S., and Mezzenga, R., "Half a century of amyloids: Past, present and future," Chem. Soc. Rev. **49**(15), 5473–5509 (2020).

Kannaian, B., Sharma, B., Phillips, M. *et al.*, "Abundant neuroprotective chaperone Lipocalin-type prostaglandin D synthase (L-PGDS) disassembles the Amyloid-β fibrils," Sci. Rep. **9**, 12579 (2019).

Kjaergaard, M., Dear, A. J., Kundel, F., Qamar, S., Meisl, G., Knowles, T. P. J., and Klenerman, D., "Oligomer diversity during the aggregation of the repeat region of Tau," ACS Chem. Neurosci. **9**(12), 3060–3071 (2018).

Knowles, T. P. and Buehler, M. J., "Nanomechanics of functional and pathological amyloid materials," Nat. Nanotechnol. **6**(8), 469–479 (2011).

Koder Hamid, M., Rüter, A., Kuczera, S., and Olsson, U., "Slow dissolution kinetics of model peptide fibrils," Int. J. Mol. Sci. **21**(20), 7671 (2020).

Lansbury, P. T. and Lashuel, H. A., "A century-old debate on protein aggregation and neurodegeneration enters the clinic," Nature **443**(7113), 774–779 (2006).

Lattanzi, C., Bernfur, K., Sparr, E., Olsson, U., and Linse, S., "Solubility of Aβ40 peptide," JCIS Open **4**, 100024 (2021).

Laughlin, R. G., *The Aqueous Phase Behavior of Surfactants* (Academic Press, London, 1994).

Lee, J. E., Sang, J. C., Rodrigues, M., Carr, A. R., Horrocks, M. H., De, S., Bongiovanni, M. N., Flagmeier, P., Dobson, C. M., Wales, D. J., Lee, S. F., and Klenerman, D., "Mapping surface hydrophobicity of α-synuclein oligomers at the nanoscale," Nano Lett. **18**(12), 7494–7501 (2018).

Lendel, C., Bjerring, M., Dubnovitsky, A., Kelly, R. T., Filippov, A., Antzutkin, O. N., Nielsen, N. C., and Härd, T., "A hexameric peptide barrel as building block of amyloid-β protofibrils," Angew. Chem., Int. Ed. **53**(47), 12756–12760 (2014).

Lifson, S. and Roig, A., "On the theory of helix—Coil transition in polypeptides," J. Chem. Phys. **34**, 1963–1974 (1961).

Lindberg, M., Axell, E., Sparr, E., and Linse, S., "A label-free high-throughput protein solubility assay and its application to Aβ40," Biophys. Chem. **307**, 107165 (2024).

Liu, Y., Zhang, Y., Sun, Y., and Ding, F., "A buried glutamate in the cross-β core renders β-endorphin fibrils reversible," Nanoscale **13**(46), 19593–19603 (2021).

Lövestam, S., Li, D., Wagstaff, J. L., Kotecha, A., Kimanius, D., McLaughlin, S. H., Murzin, A. G., Freund, S. M. V., Goedert, M., and Scheres, S. H. W., "Disease-specific tau filaments assemble via polymorphic intermediates," Nature **625**(7993), 119–125 (2024).

Löwik, D. W., Garcia-Hartjes, J., Meijer, J. T., and van Hest, J. C., "Tuning secondary structure and self-assembly of amphiphilic peptides," Langmuir **21**(2), 524–526 (2005).

Maji, S. K., Perrin, M. H., Sawaya, M. R., Jessberger, S., Vadodaria, K., Rissman, R. A., Singru, P. S., Nilsson, K. P., Simon, R., Schubert, D., Eisenberg, D., Rivier, J., Sawchenko, P., Vale, W., and Riek, R., "Functional amyloids as natural storage of peptide hormones in pituitary secretory granules," Science **325**(5938), 328–332 (2009).

Maji, S. K., Schubert, D., Rivier, C., Lee, S., Rivier, J. E., and Riek, R., "Amyloid as a depot for the formulation of long-acting drugs," PLoS Biol. **6**(2), e17 (2008).

Matson, J. B., Zha, R. H., and Stupp, S. I., "Peptide self-assembly for crafting functional biological materials," Curr. Opin. Solid State Mater. Sci. **15**(6), 225–235 (2011).

McGlinchey, R. P. and Lee, J. C., "Reversing the amyloid trend: Mechanism of fibril assembly and dissolution of the repeat domain from a human functional amyloid," Isr. J. Chem. **57**(7–8), 613–621 (2017).

Meisl, G., Yang, X., Hellstrand, E., Frohm, B., Kirkegaard, J. B., Cohen, S. I., Dobson, C. M., Linse, S., and Knowles, T. P., "Differences in nucleation behavior underlie the contrasting aggregation kinetics of the Aβ40 and Aβ42 peptides," Proc. Natl. Acad. Sci. U. S. A. **111**(26), 9384–9389 (2014).

Merrifield, R. B., "Solid phase peptide synthesis. I. The synthesis of a tetrapeptide," J. Am. Chem. Soc. **85**, 2149–2154 (1963).

Michaels, T. C. T., Šarić, A., Curk, S., Bernfur, K., Arosio, P., Meisl, G., Dear, A. J., Cohen, S. I. A., Dobson, C. M., Vendruscolo, M., Linse, S., and Knowles, T. P. J., "Dynamics of oligomer populations formed during the aggregation of Alzheimer's Aβ42 peptide," Nat. Chem. **12**(5), 445–451 (2020).

Michaels, T. C. T., Qian, D., Šarić, A., Vendruscolo, M., Linse, S., and Knowles, T. P. J., "Amyloid formation as a protein phase transition," Nat. Rev. Phys. **5**, 379–397 (2023).

Morel, B., Varela, L., and Conejero-Lara, F., "The thermodynamic stability of amyloid fibrils studied by differential scanning calorimetry," J. Phys. Chem. B **114**(11), 4010–4019 (2010).

Narimoto, T., Sakurai, K., Okamoto, A., Chatani, E., Hoshino, M., Hasegawa, K., Naiki, H., and Goto, Y., "Conformational stability of amyloid fibrils of β2-microglobulin probed by guanidine-hydrochloride-induced unfolding," FEBS Lett. **576**(3), 313–319 (2004).

Narayanan, T., Rüter, A., and Olsson, U., "Multiscale structural elucidation of peptide nanotubes by x-ray scattering methods," Front. Bioeng. Biotechnol. **9**, 654339 (2021).

Nespovitaya, N., Gath, J., Barylyuk, K., Seuring, C., Meier, B. H., and Riek, R., "Dynamic assembly and disassembly of functional β-endorphin amyloid fibrils," J. Am. Chem. Soc. **138**(3), 846–856 (2016).

Nillegoda, N. B., Kirstein, J., Szlachcic, A., Berynskyy, M., Stank, A., Stengel, F., Arnsburg, K., Gao, X., Scior, A., Aebersold, R., Guilbride, D. L., Wade, R. C., Morimoto, R. I., Mayer, M. P., and Bukau, B., "Crucial HSP70 co-chaperone complex unlocks metazoan protein disaggregation," Nature **524**(7564), 247–251 (2015).

Nilsson, M. R. and Dobson, C. M., "Chemical modification of insulin in amyloid fibrils," Protein Sci. **12**(11), 2637–2641 (2003).

Norrild, R. K., Vettore, N., Coden, A., Xue, W. F., and Buell, A. K., "Thermodynamics of amyloid fibril formation from non-equilibrium experiments of growth and dissociation," Biophys. Chem. **271**, 106549 (2021).

Nyrkova, I. A., Semenov, A. N., Aggeli, A., Bell, M., Boden, N., and McLeish, T. C. B., "Self-assembly and structure transformations in living polymers forming fibrils," Eur. Phys. J. B **17**, 499–513 (2000).

O'Nuallain, B., Shivaprasad, S., Kheterpal, I., and Wetzel, R., "Thermodynamics of Aβ(1-40) amyloid fibril elongation," Biochemistry **44**(38), 12709–12718 (2005).

Ortigosa-Pascual, L., Leiding, T., Linse, S., and Pálmadóttir, T., "Photo-induced cross-linking of unmodified α-synuclein oligomers," ACS Chem. Neurosci. **14**(17), 3192–3205 (2023).

Otzen, D. and Riek, R., "Functional amyloids," Cold Spring Harbor Perspect. Biol. **11**(12), a033860 (2019).

Padrick, S. B. and Miranker, A. D., "Islet amyloid: Phase partitioning and secondary nucleation are central to the mechanism of fibrillogenesis," Biochemistry **41**(14), 4694–4703 (2002).

Pálmadóttir, T., Waudby, C. A., Bernfur, K., Christodoulou, J., Linse, S., and Malmendal, A., "Morphology-dependent interactions between α-synuclein monomers and fibrils," Int. J. Mol. Sci. **24**(6), 5191 (2023).

Parsell, D. A., Kowal, A. S., Singer, M. A., and Lindquist, S., "Protein disaggregation mediated by heat-shock protein Hsp104," Nature **372**(6505), 475–478 (1994).

Ping, Y., Ding, D., Ramos, R. A. N. S., Mohanram, H., Deepankumar, K., Gao, J., Tang, G., and Miserez, A., "Supramolecular β-sheets stabilized protein nanocarriers for drug delivery and gene transfection," ACS Nano **11**(5), 4528–4541 (2017).

Pronchik, J., He, X., Giurleo, J. T., and Talaga, D. S., "In vitro formation of amyloid from alpha-synuclein is dominated by reactions at hydrophobic interfaces," J. Am. Chem. Soc. **132**(28), 9797–9803 (2010).

Qiang, W., Kelley, K., and Tycko, R., "Polymorph-specific kinetics and thermodynamics of β-amyloid fibril growth," J. Am. Chem. Soc. **135**(18), 6860–6871 (2013).

Raman, B., Chatani, E., Kihara, M., Ban, T., Sakai, M., Hasegawa, K., Naiki, H., Rao, C., and Goto, Y., "Critical balance of electrostatic and hydrophobic interactions is required for β_2-microglobulin amyloid fibril growth and stability," Biochemistry **44**(4), 1288–1299 (2005).

Rezaei-Ghaleh, N., Amininasab, M., Kumar, S., Walter, J., and Zweckstetter, M., "Phosphorylation modifies the molecular stability of β-amyloid deposits," Nat. Commun. **7**, 11359 (2016).

Rodriguez Camargo, D. C., Chia, S., Menzies, J., Mannini, B., Meisl, G., Lundqvist, M., Pohl, C., Bernfur, K., Lattanzi, V., Habchi, J., Cohen, S. I., Knowles, T. P. J., Vendruscolo, M., and Linse, S., "Surface-catalyzed secondary nucleation dominates the generation of toxic IAPP aggregates," Front. Mol. Biosci. **8**, 757425 (2021a).

Rodriguez Camargo, D. C., Sileikis, E., Chia, S., Axell, E., Bernfur, K., Cataldi, R. L., Cohen, S. I. A., Meisl, G., Habchi, J., Knowles, T. P. J., Vendruscolo, M., and Linse, S., "Proliferation of Tau 304-380 fragment aggregates through autocatalytic secondary nucleation," ACS Chem. Neurosci. **12**(23), 4406–4415 (2021b).

Romero, D., Aguilar, C., Losick, R., and Kolter, R., "Amyloid fibers provide structural integrity to Bacillus subtilis biofilms," Proc. Natl. Acad. Sci. U. S. A. **107**(5), 2230–2234 (2010).

Ruschak, A. M. and Miranker, A. D., "Fiber-dependent amyloid formation as catalysis of an existing reaction pathway," Proc. Natl. Acad. Sci. U. S. A. **104**(30), 12341–12346 (2007).

Rüter, A., Kuczera, S., Pochan, D. J., and Olsson, U., "Twisted ribbon aggregates in a model peptide system," Langmuir **35**(17), 5802–5808 (2019).

Rüter, A., Kuczera, S., Stenhammar, J., Zinn, T., Narayanan, T., and Olsson, U., "Tube to ribbon transition in a self-assembling model peptide system," Phys. Chem. Chem. Phys. **22**(33), 18320–18327 (2020).

Röder, C., Vettore, N., Mangels, L. N., Gremer, L., Ravelli, R. B. G., Willbold, D., Hoyer, W., Buell, A. K., and Schröder, G. F., "Atomic structure of PI3-kinase SH3 amyloid fibrils by cryo-electron microscopy," Nat. Commun. **10**(1), 3754 (2019).

Saad, S., Cereghetti, G., Feng, Y., Picotti, P., Peter, M., and Dechant, R., "Reversible protein aggregation is a protective mechanism to ensure cell cycle restart after stress," Nat. Cell Biol. **19**(10), 1202–1213 (2017).

Sawada, M., Yamaguchi, K., Hirano, M., Noji, M., So, M., Otzen, D., Kawata, Y., and Goto, Y., "Amyloid formation of alpha-synuclein based on the solubility- and supersaturation-dependent mechanism," Langmuir **36**(17), 4671–4681 (2020).

Selkoe, D. J., "Cell biology of protein misfolding: The examples of Alzheimer's and Parkinson's diseases," Nat. Cell Biol. **6**(11), 1054–1061 (2004).

Semenov, A. N. and Subbotin, A. V., "Theory of self-assembling structures of model oligopeptides," Macromolecules **43**(7), 3487–3501 (2010).

Sevigny, J., Chiao, P., Bussière, T., Weinreb, P. H., Williams, L., Maier, M., Dunstan, R., Salloway, S., Chen, T., Ling, Y., O'Gorman, J., Qian, F., Arastu, M., Li, M., Chollate, S., Brennan, M. S., Quintero-Monzon, O., Scannevin, R. H., Arnold, H. M., Engber, T., Rhodes, K., Ferrero, J., Hang, Y., Mikulskis, A., Grimm, J., Hock, C., Nitsch, R. M., and Sandrock, A., "The antibody aducanumab reduces Aβ plaques in Alzheimer's disease," Nature **537**(7618), 50–56 (2016).

Shammas, S. L., Knowles, T. P., Baldwin, A. J., Macphee, C. E., Welland, M. E., Dobson, C. M., and Devlin, G. L., "Perturbation of the stability of amyloid fibrils through alteration of electrostatic interactions," Biophys. J. **100**(11), 2783–2791 (2011).

Shimanovich, U., Levin, A., Eliaz, D., Michaels, T., Toprakcioglu, Z., Frohm, B., De Genst, E., Linse, S., Åkerfeldt, K. S., and Knowles, T. P. J., "pH-responsive capsules with a fibril scaffold shell assembled from an amyloidogenic peptide," Small **17**(26), e2007188 (2021).

Shukla, H., Kumar, R., Sonkar, A., Mitra, K., Akhtar, M. S., and Tripathi, T., "Salt-regulated reversible fibrillation of Mycobacterium tuberculosis isocitrate lyase: Concurrent restoration of structure and activity," Int. J. Biol. Macromol. **104**(Pt A), 89–96 (2017).

Sil, T. B., Sahoo, B., Bera, S. C., and Garai, K., "Quantitative characterization of metastability and heterogeneity of amyloid aggregates," Biophys. J. **114**(4), 800–811 (2018).

Sims, J. R., Zimmer, J. A., Evans, C. D., Lu, M., Ardayfio, P., Sparks, J., Wessels, A. M., Shcherbinin, S., Wang, H., Monkul Nery, E. S., Collins, E. C., Solomon, P., Salloway, S., Apostolova, L. G., Hansson, O., Ritchie, C., Brooks, D. A., Mintun, M., Skovronsky, D. M., and TRAILBLAZER-ALZ 2 Investigators, "Donanemab in early symptomatic alzheimer disease: The TRAILBLAZER-ALZ 2 randomized clinical trial," JAMA **330**(6), 512–527 (2023).

Shorter, J., "The mammalian disaggregase machinery: Hsp110 synergizes with Hsp70 and Hsp40 to catalyze protein disaggregation and reactivation in a cell-free system," PLoS One **6**(10), e26319 (2011).

Sipe, J. D., Benson, M. D., Buxbaum, J. N., Ikeda, S., Merlini, G., Saraiva, M. J., and Westermark, P., "Amyloid fibril protein nomenclature: 2012 recommendations from the Nomenclature Committee of the International Society of Amyloidosis," Amyloid **19**(4), 167–170 (2012).

Sneideris, T., Milto, K., and Smirnovas, V., "Polymorphism of amyloid-like fibrils can be defined by the concentration of seeds," PeerJ **3**, e1207 (2015).

Sudhakar, S. and Mani, E., "Rapid dissolution of amyloid β fibrils by silver nanoplates," Langmuir **35**(21), 6962–6970 (2019).

Sun, J. E., Stewart, B., Litan, A., Lee, S. J., Schneider, J. P., Langhans, S. A., and Pochan, D. J., "Sustained release of active chemotherapeutics from injectable-solid β-hairpin peptide hydrogel," Biomater. Sci. **4**(5), 839–848 (2016).

Takeda, T. and Klimov, D. K., "Temperature-induced dissociation of Aβ monomers from amyloid fibril," Biophys. J. **95**(4), 1758–1772 (2008).

Tipping, K. W., Karamanos, T. K., Jakhria, T., Iadanza, M. G., Goodchild, S. C., Tuma, R., Ranson, N. A., Hewitt, E. W., and Radford, S. E., "pH-induced molecular shedding drives the formation of amyloid fibril-derived oligomers," Proc. Natl. Acad. Sci. U. S. A. **112**(18), 5691–5696 (2015).

Tolman, R. C., "The principle of microscopic reversibility," Proc. Natl. Acad. Sci. U. S. A. **11**(7), 436–439 (1925).

Torrent, J., Alvarez-Martinez, M. T., Liautard, J. P., and Lange, R., "Modulation of prion protein structure by pressure and temperature," Biochim. Biophys. Acta **1764**(3), 546–551 (2006).

Ulijn, R. V. and Smith, A. M., "Designing peptide based nanomaterials," Chem. Soc. Rev. **37**(4), 664–675 (2008).

van den Heuvel, M., Löwik, D. W., and van Hest, J. C., "Self-assembly and polymerization of diacetylene-containing peptide amphiphiles in aqueous solution," Biomacromolecules **9**(10), 2727–2734 (2008).

van Dyck, C. H., Swanson, C. J., Aisen, P., Bateman, R. J., Chen, C., Gee, M., Kanekiyo, M., Li, D., Reyderman, L., Cohen, S., Froelich, L., Katayama, S., Sabbagh, M., Vellas, B., Watson, D., Dhadda, S., Irizarry, M., Kramer, L. D., and Iwatsubo, T., "Lecanemab in early Alzheimer's disease," N. Engl. J. Med. **388**(1), 9–21 (2023).

Vettore, N. and Buell, A. K., "Thermodynamics of amyloid fibril formation from chemical depolymerization," Phys. Chem. Chem. Phys. **21**(47), 26184–26194 (2019).

Vemula, P., Schoch, K. M., and Miller, T. M., "Evaluating the efficacy of purchased antisense oligonucleotides to reduce mouse and human tau *in vivo*," Front. Mol. Neurosci. **16**, 1320182 (2023).

Wang, J., Liu, K., Xing, R., and Yan, X., "Peptide self-assembly: Thermodynamics and kinetics," Chem. Soc. Rev. **45**(20), 5589–5604 (2016).

Wei, G., Su, Z., Reynolds, N. P., Arosio, P., Hamley, I. W., Gazit, E., and Mezzenga, R., "Self-assembling peptide and protein amyloids: From structure to tailored function in nanotechnology," Chem. Soc. Rev. **46**(15), 4661–4708 (2017).

Wei, J., Meisl, G., Dear, A., Oosterhuis, M., Melki, R., Emanuelsson, C., Linse, S., and Knowles, T. P. J., "Kinetic models reveal the interplay of protein production and aggregation," Chem. Sci. **15**(22), 8430–8442 (2024).

Wentink, A. S., Nillegoda, N. B., Feufel, J., Ubartaitė, G., Schneider, C. P., De Los Rios, P., Hennig, J., Barducci, A., and Bukau, B., "Molecular dissection of amyloid disaggregation by human HSP70," Nature **587**(7834), 483–488 (2020).

Wetzel, R., "Kinetics and thermodynamics of amyloid fibril assembly," Acc. Chem. Res. **39**(9), 671–679 (2006).

White, D. A., Buell, A. K., Dobson, C. M., Welland, M. E., and Knowles, T. P., "Biosensor-based label-free assays of amyloid growth," FEBS Lett. **583**(16), 2587–2592 (2009).

Wilkinson, M., Xu, Y., Thacker, D., Taylor, A. I. P., Fisher, D. G., Gallardo, R. U., Radford, S. E., and Ranson, N. A., "Structural evolution of fibril polymorphs during amyloid assembly," Cell **186**(26), 5798–5811.e26 (2023).

Wördehoff, M. M., Shaykhalishahi, H., Groß, L., Gremer, L., Stoldt, M., Buell, A. K., Willbold, D., and Hoyer, W., "Opposed effects of dityrosine formation in soluble and aggregated α-synuclein on fibril growth," J. Mol. Biol. **429**(20), 3018–3030 (2017).

Zhang, S., "Discovery and design of self-assembling peptides," Interface Focus **7**, 20170028 (2017).

Zhou, J., Li, T., Peydayesh, M., Usuelli, M., Lutz-Bueno, V., Teng, J., Wang, L., and Mezzenga, R., "Oat plant amyloids for sustainable functional materials," Adv. Sci. **9**(4), e2104445 (2022).

Zimm, B. H. and Bragg, J. K., "Theory of the phase transition between helix and random coil in polypeptide chains," J. Chem. Phys. **31**(2), 526–531 (1959).